



### **Science Arts & Métiers (SAM)**

is an open access repository that collects the work of Arts et Métiers Institute of Technology researchers and makes it freely available over the web where possible.

This is an author-deposited version published in: <https://sam.ensam.eu>  
Handle ID: <http://hdl.handle.net/10985/17957>

#### **To cite this version :**

Konstantinos KALLITSIS, Thibaut SOULESTIN, Sylvie TENCÉ-GIRAULT, Cyril BROCHON, Éric CLOUTET, Fabrice DOMINGUES-DOS SANTOS, Georges HADZIOANNOU - Introducing Functionality to Fluorinated Electroactive Polymers - Macromolecules - Vol. 52, n°21, p.8503-8513 - 2019

Any correspondence concerning this service should be sent to the repository

Administrator : [scienceouverte@ensam.eu](mailto:scienceouverte@ensam.eu)



# Introducing Functionality to Fluorinated Electroactive Polymers

Konstantinos Kallitsis,<sup>†</sup> Thibaut Soulestin,<sup>‡,‡</sup> Sylvie Tencé-Girault,<sup>§,||</sup> Cyril Brochon,<sup>†,‡</sup> Eric Cloutet,<sup>†,‡</sup> Fabrice Domingues Dos Santos,<sup>‡</sup> and Georges Hadziioannou<sup>\*,†,‡,‡</sup>

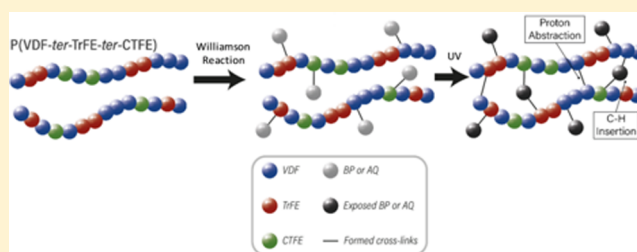
<sup>†</sup>Laboratoire de Chimie des Polymères Organiques (LCPO UMR 5629), CNRS-Université de Bordeaux-Bordeaux INP, 16 Avenue Pey-Berland, 33607 Pessac Cedex, France

<sup>‡</sup>Arkema-Piezotech, Rue Henri-Moissan, 69493 Pierre-Benite Cedex, France

<sup>§</sup>PIMM, Arts et Metiers Institute of Technology, CNRS, Cnam, HESAM University, boulevard de l'Hopital, 75013 Paris, France

<sup>||</sup>Arkema, CERDATO, Route du Rilsan, 27470 Serquigny, France

**ABSTRACT:** Fluorinated electroactive polymers (FEPs) are among the most interesting insulating materials for the production of organic electronic devices. Their ability to tune their response to an applied electric field makes them appropriate for vastly different applications in electronics. However, due to the chemical inertness of such polymers and the rather complex synthetic processes required for their production, introducing additional functionality to FEPs remains an open challenge. Here, we present a facile way to introduce additional functionality to FEPs and more specifically photopatternability by a simple etherification method, which allows us to introduce almost any functional group on FEPs. Photo-cross-linkable moieties were introduced on FEPs using this method, inducing photopatternability, while tuning their electroactive response with great property enhancement up to 60% in terms of relative permittivity in several cases.



## ■ INTRODUCTION

If flexible organic electronics are to be realized in a massive scale, three classes of materials ought to be optimized. These classes are conductors, semiconductors, and insulators, which are the three essential components for any electronic device. Organic conductors<sup>1</sup> and semiconductors<sup>2</sup> have been extensively developed over the past 40 years, while research on insulators with a high dielectric constant and thus high performance is lagging far behind. Fluorinated electroactive polymers (FEPs) are perhaps the most prominent class of insulating polymers and are attracting increasingly high interest both in industrial and laboratory fields.<sup>3</sup> Poly(vinylidene fluoride) (PVDF) and its copolymers dominate this group due to their excellent dielectric properties as well as their chemical and mechanical stability. Furthermore, their electroactive properties, varying from ferroelectric<sup>4</sup> to relaxor-ferroelectric,<sup>5</sup> significantly increase their scope of application. Due to the difficulty in controlling the synthesis of such polymers, adding further functionality, although essential to broaden their application, still remains an open challenge.<sup>6,7</sup> Some efforts toward this direction have been recently demonstrated by the preparation of block copolymers of P(VDF-co-TrFE) with polystyrene or poly(2-vinyl-pyridine) to tailor the electroactive response from ferroelectric to relaxor-ferroelectric and linear dielectric.<sup>6</sup> Despite the very interesting findings, a large increase in leakage current was observed for the prepared polymers, creating a main bottleneck for their potential application. Also, the used

solution polymerization processes for the polymerization of VDF and TrFE make that approach noncompatible with industrial standards that rely exclusively on miniemulsion<sup>8</sup> or suspension<sup>9</sup> polymerizations in aqueous media. In other attempts to tune the electroactive properties of FEPs, grafting strategies have been explored, where side chains appear to induce antiferroelectric-like behavior to the electroactive polymers, by providing an insulating layer to the ferroelectric crystals.<sup>10,11</sup> However, the controlled radical polymerization (ATRP) process used in these cases makes them unattractive for industrial scale as extensive purification steps to remove all copper residues can significantly increase the production costs. Grafting of a polymer chain containing highly polarizable hydroxyl (OH) groups has been reported to have positive impact both on the dielectric and ferroelectric properties of PVDF-based fluoropolymers,<sup>12</sup> limited only by an increased leakage current and a decrease in crystallinity.

An effort to introduce additional functionality to the electroactive properties, and more specifically photopatternability, has been recently reported by our group.<sup>13</sup> In this approach, photosensitive azide groups were grafted on relaxor-ferroelectric P(VDF-ter-TrFE-ter-CTFE), making it photo-cross-linkable while maintaining its electroactive properties. These polymers were used as negative photoresists

in a photolithographic process, broadening the scope of application of FEPs. Despite all of the advantages that this approach brought, some limitations hinder its potential for commercialization. First, this approach provided a specific tool to graft azide groups on CTFE containing fluoropolymers, but no flexibility in terms of the grafted group was possible. The second and maybe even more important limitation is that cross-linking appears to have a detrimental impact on both the dielectric and ferroelectric properties of these polymers. Finally, the azide chemistry is also quite restricted at the industrial level.

We were thus looking for an alternative approach that would allow us to introduce functionality on FEPs while being versatile as the grafted group and ideally maintaining or even enhancing the electroactive properties.

## ■ EXPERIMENTAL SECTION

**Materials.** Unless otherwise stated, all chemicals were purchased from Acros Organics or Merck Chemicals and used without any further purification. The statistical terpolymers P(VDF-*ter*-TrFE-*ter*-CTFE) were provided by Arkema-Piezotech (France). Argon was supplied by Air Liquid with at least 99.99% purity.

**Synthesis.** Typical modification reactions were performed using standard Schlenk techniques. For the 4-hydroxy benzophenone grafting reaction on P(VDF-*ter*-TrFE-*ter*-CTFE) (61.7/28.3/10), 1 g of terpolymer was dissolved in 25 mL of acetone in a 50 mL glass Schlenk ampoule. 4-Hydroxy benzophenone (0.8 g, 4.0 mmol) and potassium carbonate (0.7 g, 5.6 mmol) were mixed in acetone (15 mL). The glass Schlenk ampoule was sealed under argon and heated to 60 °C in the dark for 1 h. Then, the second solution was filtered and added to the first to remove the excess of the base. The glass ampoule was sealed and left in the dark at 60 °C for 16 h to react. A few drops of condensed HCl were added after the end of the reaction, and the polymer was precipitated in water and washed with water, ethanol, and chloroform for several hours to remove any impurities. Then, it was dried in a vacuum oven at 40 °C for 12 h.

For the 2-hydroxy anthraquinone grafting reaction on P(VDF-*ter*-TrFE-*ter*-CTFE) (61.7/28.3/10), 5 g of terpolymer were dissolved in 100 mL of dimethyl formamide (DMF) in a 250 mL glass Schlenk ampoule. 2-Hydroxy anthraquinone (1.4 g, 6.4 mmol) and potassium carbonate (1.32, 9.6 mmol) were mixed in dimethyl formamide (DMF) (100 mL). The glass Schlenk ampoule was sealed under argon and heated to 80 °C in the dark for 1 h. Then, the second solution was filtered and added to the first to remove the excess of the base. The glass ampoule was sealed and left in the dark at 80 °C for 16 h to react. The polymer was precipitated in water and then washed with water, ethanol, and chloroform for several hours to remove any impurities. Then, it was dried in a vacuum oven at 40 °C for 12 h.

**Instruments and Characterization.** <sup>1</sup>H NMR and <sup>19</sup>F NMR spectra were recorded on a Bruker Advance DPX 400 MHz spectrometer. All samples were prepared in deuterated acetone (*d*<sub>6</sub>). FT-IR spectra were recorded on a Bruker Vertex 70 using diamond ATR spectroscopy. The differential scanning calorimetry (DSC) thermograms were recorded by a TA Instruments DSC Q100 RCS. The DSC analysis was performed from 0 to 200 °C at a heating or cooling rate of 10 °C/min. A first heating ramp was used to erase the thermal history and solvents traces of the polymer powders while the first cooling and second heating ramps were recorded. Broadband dielectric spectroscopy of metal–polymer–metal devices was performed on a Solartron 1260 A impedance analyzer. Displacement hysteresis loops of the metal–polymer–metal devices were recorded at room temperature using a TF analyzer 2000E from aixACCT Systems. A continuous triangular wave with a frequency of 10 Hz was used. UV–visible absorption spectra were recorded on self-standing films using a Shimadzu spectrophotometer UV-3600. Atomic force microscopy (AFM) was performed on spin-coated polymer films by a Dimension Fast Scan from Bruker in tapping

mode. Photolithography was performed on an EVG6200 mask aligner. Film thicknesses were measured by a Bruker Dektak XT-A stylus profilometer.

Simultaneous SAXS–WAXS experiments were performed on a Xenocs Nano-inXider SW system in transmission mode using Cu K $\alpha$  radiation ( $\lambda = 1.54$  Å) from an X-ray microsource (GeniX3D) operating at 50 kV and 0.6 mA (30 W). Scattering patterns were collected using the combination of two detectors Pilatus3 (Dectris) operating simultaneously in SAXS and WAXS positions. Distances between the sample and SAXS and WAXS detectors are fixed allowing a continuous *q* range between 0.005 and 4.2 Å<sup>−1</sup> ( $2\theta$  range between 0.07 and 62°). The SAXS and WAXS profiles are treated to extract structural quantitative values: the long period, *L<sub>p</sub>*, the interplanar distances, *d*, and the crystallinity,  $\chi_c$ . We have already published<sup>14</sup> the detailed procedure used for the SAXS–WAXS quantitative analysis.

**Preparation of Patterned Thin Films.** For benzophenone containing P(VDF-*ter*-TrFE-*ter*-CTFE), a 4 wt % solution of the benzophenone-modified polymer (4.4%) in cyclopentanone was spin-coated on a silicon wafer at 500 rpm for 5 s and then at 1000 rpm for 1 min, yielding a 250 nm-thick film. The wafer was soft-baked before exposure at 130 °C for 5 min and subsequently cross-linked by UV light under nitrogen, using a photolithographic mask. The applied UV dose was 6 J/cm<sup>2</sup>. Then, the film was postexposure baked at 130 °C for 5 min. Finally, the patterned film was developed in a blend of one-fifth cyclopentanone and four-fifths isopropanol for 1 min. Subsequently, the wafer was rinsed with isopropanol and dried with compressed air.

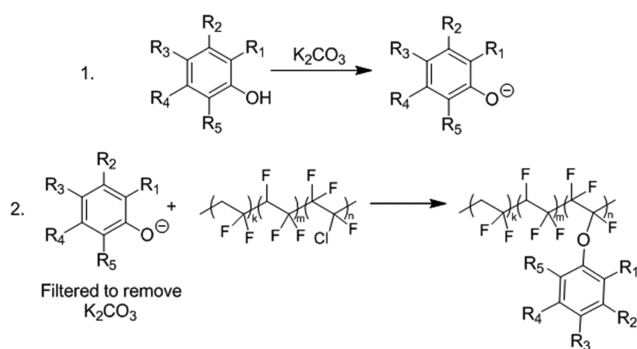
For anthraquinone containing P(VDF-*ter*-TrFE-*ter*-CTFE), a 4 wt % solution of the anthraquinone-modified polymer (0.6%) in cyclopentanone was spin-coated on a silicon wafer at 500 rpm for 5 s and then at 1000 rpm for 1 min, yielding a 250 nm-thick film. The wafer was soft-baked before exposure at 250 °C for 5 min and subsequently cross-linked by UV light under nitrogen, using a photolithographic mask. The applied UV dose was 3 J/cm<sup>2</sup>. Then, the film was postexposure baked at 250 °C for 5 min. Finally, the patterned film was developed in a blend of one-fifth cyclopentanone and four-fifths isopropanol for 1 min. Subsequently, the wafer was rinsed with isopropanol and dried with compressed air.

**Device Fabrication.** The metal–polymer–metal devices were fabricated as follows. Glass substrates were cleaned and sonicated in acetone and isopropanol for 15 min. Then, a layer of aluminum (80 nm) was evaporated as the bottom electrode using a thermal evaporator at a pressure of  $1 \times 10^{-6}$  mbar. Subsequently a 10 wt % solution polymer dielectric layer was spin-coated at 500 rpm for 5 s and at then 1000 rpm for 1 min. An aluminum top electrode (80 nm) was evaporated, creating a metal–insulator–metal device with an area of 2 mm<sup>2</sup>. The devices were annealed at 110 °C for 1 h and allowed to cool down slowly to room temperature.

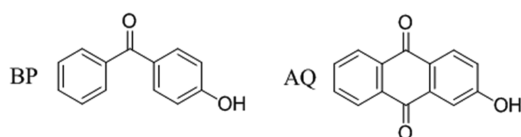
## ■ RESULTS AND DISCUSSION

**Synthesis and Chemical Characterization.** To make the grafting of different groups on FEPs possible, we developed a simple etherification reaction that would allow the grafting of any phenol containing functional group on the fluoropolymer's backbone. Similar approaches have been reported in the literature for the modification of non-electroactive fluorinated polymers such as CTFE containing fluoropolymers.<sup>15</sup> In our opinion, one of the main difficulties in developing such method is the use of bases to activate the phenol group since FEPs are known to be prone to dehydrofluorination in the presence of bases.<sup>16</sup> To overcome this bottleneck, we introduced a two-step approach (Scheme 1) in which the phenol containing functional group is treated with a base separately to activate the phenols and then transferred after filtration<sup>17</sup> into a solution of fluoropolymer, where the reaction occurs, while minimizing the effect of dehydrofluorination.

**Scheme 1. Two-Step Etherification Reaction of Functionalized Phenols on P(VDF-*ter*-TrFE-*ter*-CTFE):** First, the Phenol is Deprotonated with the Use of a Base and Subsequently Filtered in a Solution of the Polymer, where the Substitution and thus the Grafting Occur



**Scheme 2. Chemical Structures of 4-Hydroxy Benzophenone (BP) and 2-Hydroxy Anthraquinone (AQ)**



Since making fluoropolymers compatible with photolithography is a topic of increasingly high interest to broaden their scope of application, we decided to graft hydroxy-functionalized photoinitiators on the fluoropolymers to make them photo-cross-linkable. We chose to use two different photoinitiator molecules, namely, benzophenone (BP) and

anthraquinone (AQ), as polymers bearing these molecules as side groups have been reported in literature to cross-link spontaneously upon exposure to UV light and thus act as negative photoresists.<sup>18,19</sup> The hydroxy-functionalized photoinitiators are shown in Scheme 2.

Fluoropolymers with different grafting degrees of the two photoinitiators were synthesized by varying the feeding ratios. All of the synthesized polymers were characterized by <sup>1</sup>H and <sup>19</sup>F NMR as well as FT-IR spectra, as shown in Figures 1, S1 and S3. The presence of the aromatic photoinitiator (PI) led to the appearance of the signals at 7–8 ppm in the <sup>1</sup>H NMR spectra (Figure 1a,c), which was then used to calculate the grafting degrees. New bands were also observed in the FT-IR spectra (Figure 1b,d), indicating the presence of the C–H and C=O groups of the photoinitiators with progressively increasing intensity with the PI content. At the same time, the appearance of unsaturation was observed in both FT-IR (Figure 1b,d) with the band at 1720 cm<sup>−1</sup> and <sup>1</sup>H NMR (Figure 1a,c) with the appearance of signals at 6–6.7 ppm and <sup>19</sup>F NMR spectra (Figures S1 and S3). The absence of any –OH traces both in the FT-IR and NMR spectra strongly suggests that all of the PI groups are successfully grafted on the fluoropolymer chain. This was further verified by size exclusion chromatography (Figures S2 and S4), where, while the pristine fluoropolymer has no absorption in the UV detector, the fluoropolymer grafted with photoinitiators absorbs in UV, confirming that the grafting reaction was successful.

The grafting degrees were calculated from the <sup>1</sup>H NMR spectra using the following equation and are gathered in Table 1.

$$\text{grafting degree} = \frac{\int_{7\text{ppm}}^{8\text{ppm}} \text{aromatic protons} / \text{number of protons per PI}}{\int_{5\text{ppm}}^{6\text{ppm}} \text{CHF of TrFE} + (\int_{2.2\text{ppm}}^{3.7\text{ppm}} \text{CH}_2 \text{ of VDF}) / 2 + (\int_{6\text{ppm}}^{6.7\text{ppm}} \text{CH of double bonds}) \times 2}$$

As discussed above, in addition to the desired substitution reaction, unsaturation was also created on the fluoropolymer backbone (Scheme 3) due to the basic nature of the used phenoxides. The amount of double bonds was calculated for each polymer from the <sup>1</sup>H NMR spectra, as shown in Figure 1. The double bond contents are presented in Table 1. In all cases, a considerable amount of double bonds was created; however, the polymers maintained their solubility in common solvents such as cyclopentanone and dimethyl formamide (DMF) and that is mostly attributed to the two-step process that was followed, which included the filtration of the base.

In the cases that the base was not filtered off, the polymers would become black and lose their solubility.

**Structure and Morphology Characterization.** As the desired electroactive properties are known to derive from the crystalline state of these terpolymers,<sup>20,21</sup> differential scanning calorimetry (DSC) was used to get a first estimation of the effect that the modification reactions have on the polymer crystallinity. After a first heating, we observed from the first cooling ramp (Figure 2a,c) that when the grafting degree was small (≤0.6%) the crystallization peak becomes sharper for both photoinitiators, indicating more homogeneous crystal

**Table 1. Reaction Conditions and <sup>1</sup>H NMR Data for P(VDF-*ter*-TrFE-*ter*-CTFE) Grafted with Benzophenone (BP) and Anthraquinone (AQ) Groups**

	equivalents of PI	reaction time	TrFE (1 H) 4.7–5.7 ppm	double bonds (1 H) 6–7 ppm	aromatic 7–8 ppm	grafting degree
BP	(1) 0	0 h	28.3	0%	0	0%
	(2) 0.3	4 h	28.3	7.3%	3.7 (9 H)	0.4%
	(3) 0.5	4 h	28.3	7.1%	9.2 (9 H)	1%
	(4) 0.5	3 days	28.3	18%	59 (9 H)	6.5%
AQ	(2) 0.1	3 days	28.3	6.2%	4.4 (8 H)	0.6%
	(3) 0.3	3 days	28.3	8.6%	18.4 (8 H)	2.3%
	(4) 0.5	1 day	28.3	14.6%	46 (8 H)	6%

**Scheme 3. Reaction of the Fluoropolymer with the Base, Leading to the Formation of Unsaturation on the Polymer Backbone**

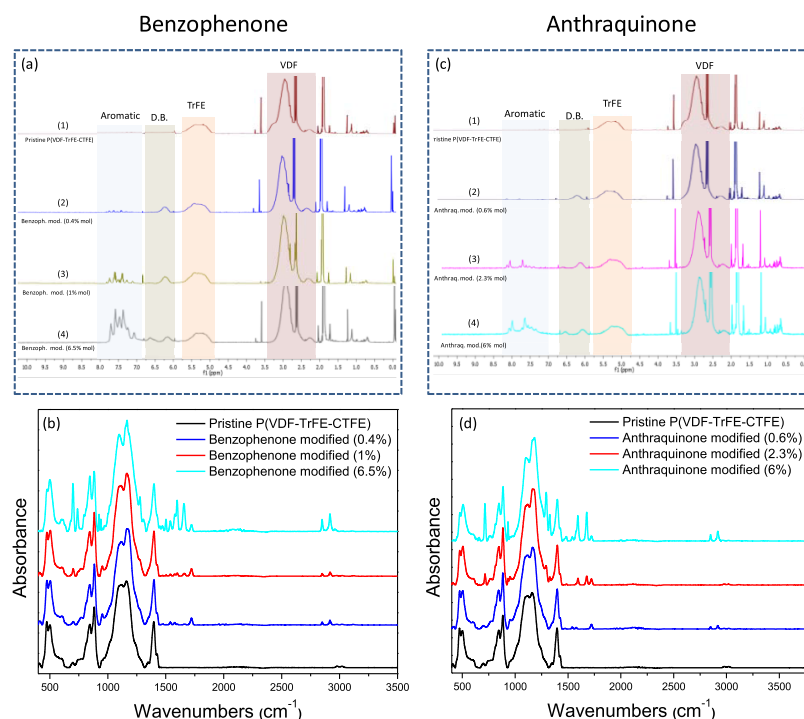
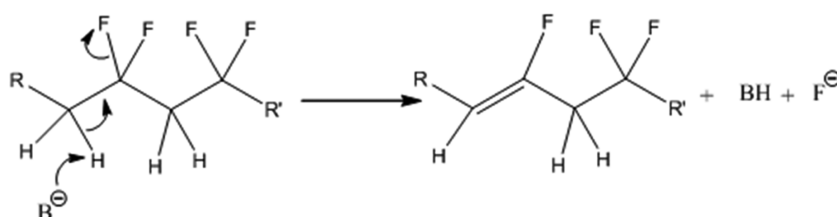


**Figure 1.**  $^1\text{H}$  NMR (400 MHz, acetone- $d_6$ ) (a, c) and ATR FT-IR (b, d) spectra of P(VDF-*ter*-TrFE-*ter*-CTFE) grafted with different benzophenone (a, b) and anthraquinone (c, d) contents.

size distribution, while being approximately at the same temperature as the peak of the pristine polymer, which is an indicator of a similar nucleation process. However, with increasing the grafting degree, the crystallization peak shifts to a lower temperature and for certain contents and above it totally disappears, indicating a progressive hindering of crystallization. During the second heating ramp, we observe a significant decrease of the melting enthalpy after grafting and a small decrease of the melting temperature for grafting degree higher than 1%. The quantitative data derived for the DSCs are presented in Table 2.

To understand the evolution of the crystalline phases with the chemical modification, we performed simultaneous SAXS–WAXS experiments on films as cast and after 1 h annealing at 110 °C, below the melting temperature. Regardless of the modification degree, WAXS spectra (Figure 3) exhibit a main Bragg peak at  $2\theta = 18^\circ$  superimposed on a broad signal associated to the amorphous phase. This Bragg peak is associated with the interplanar distances of the RFE orthorhombic pseudohexagonal phase described in a previous work.<sup>14</sup> When the degree of modification increases, the intensity of the RFE Bragg peak decreases considerably. Furthermore, the peak becomes asymmetric and it shifts toward higher  $2\theta$  angles. After annealing at 110 °C, below the

melting temperature, an increase of the Bragg peak intensity is observed.

The spectra are decomposed into broad and sharp peaks associated with amorphous and crystalline phases, respectively (Figure 3d). Two crystalline peaks are sometimes needed to refine the main peak; these are the orange and blue ones. The Bragg peak, at around  $18^\circ$ , is associated with interplanar distances perpendicular to the chain direction; it corresponds to the juxtaposition of two diffraction lines coming from the (200) and (110) planes of the pseudohexagonal structure. The width of this peak is due to both the separation of the two peaks  $d_{200}$  and  $d_{110}$  and the extension of the crystal.<sup>14</sup> The black peak at around  $2\theta = 40^\circ$  corresponds to the juxtaposition of several Bragg peaks mostly characteristic of the order along the chains.<sup>22</sup> The interplanar distance,  $d$ , and the width,  $\Delta 2\theta$ , of the main Bragg peak are reported in Table 3 along with the crystallinity,  $\chi_c$ .

Chemical modification with benzophenone (BP) or anthraquinone (AQ) induces a decrease of the interplanar distance perpendicular to the chain direction and a thinning of the diffraction line. We deduce that the pendent groups, BP or AQ, are not incorporated in the crystalline phase. However, surprisingly, crystallinity does not decrease for a small amount of modification, less than 2%. However, for a

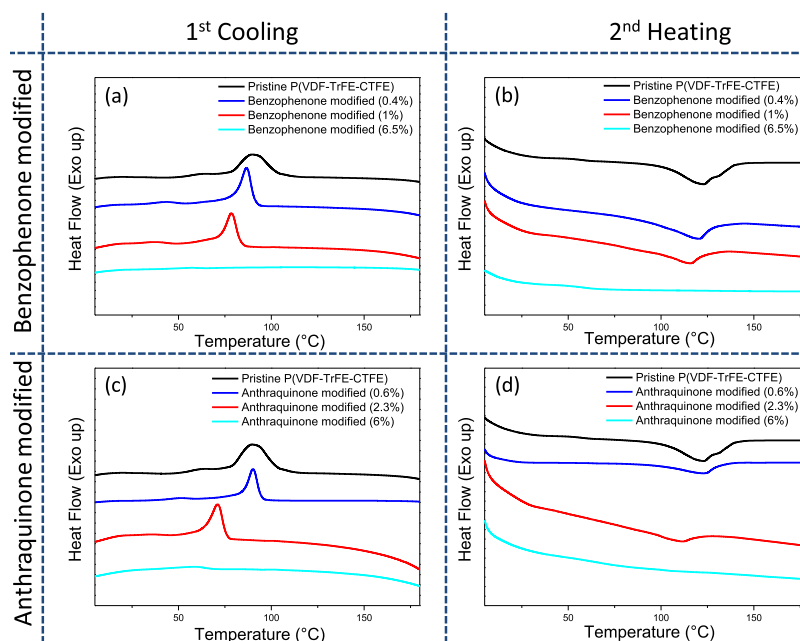


**Figure 2.** DSC thermograms showing the first cooling (a, c) and second heating (b, d) of P(VDF-*ter*-TrFE-CTFE) grafted with different benzophenone (a, b) and anthraquinone (c, d) contents.

**Table 2. Summary of the Data Obtained by Differential Scanning Calorimetry of Pristine, BP, and AQ-Modified PVDF-TrFE-CTFE Terpolymer**

as synthesized samples	crystallization		melting	
	temperature (°C)	enthalpy (J/g)	temperature (°C)	enthalpy (J/g)
pristine terpolymer	90	13	123	14
benzophenone (0.4%)	87	12	120	8
benzophenone (1%)	79	9	116	5
benzophenone (6.5%)				
anthraquinone (0.6%)	90	12	123	10
anthraquinone (2.3%)	71	7	110	3
anthraquinone (6%)	59	0.9		

high degree of chemical modification (>2%), a decrease of the crystallinity and a broadening of the Bragg peak are observed, showing the degradation of the crystalline order. The thinning of the peak can be interpreted as an extension of the correlation length in the crystalline lamellae plane or as a small change of the crystalline cell toward the hexagonal phase.

The Lorentz-corrected SAXS spectra (Figure 4) show the evolution of the crystalline lamellae periodicity after chemical modifications and after annealing. From the maximum of these profiles, we deduced the period of the crystalline lamellae,  $L_p$ ; this value is reported in Table 3.

We observe a significant decrease of  $L_p$  when the amount of chemical modification increases. This decrease is explained by the nonincorporation of the pendent group in the crystalline lamellae, leading to a decrease of the crystalline lamella thickness. At the same time, the intensity increases due to an increase of the contrast between crystalline and

amorphous lamellae. Pendent groups localized at the crystalline and amorphous interface and in the amorphous phase modify the electronic density and then the contrast.

After annealing, a major reorganization of the crystalline lamellae is observed with a significant increase of  $L_p$  and the appearance of well-defined second-order diffraction peak. For the lowest chemical modifications, 0.4% BP and 0.6% AQ, the long periods,  $L_p$ , are comparable with the period of the unmodified terpolymer. Only the intensity differs, as the crystallinities are comparable (23–24%), we conclude on differences in electronic density and/or in localization of BP or AQ pendent groups.

To visualize the effect that the modification has on the morphology of the polymers, spin-coated films prepared with the anthraquinone-modified fluoropolymers were characterized by atomic force microscopy (AFM) in tapping mode. The phase images, shown in Figure 5, confirm that for a low anthraquinone content (0.6%) the terpolymer's rod-like crystalline domains become larger with more homogeneous size distribution (Figure 5b). However, when the anthraquinone content increases to 2.3%, the morphology become granular, the domain size become much smaller (Figure 5c), and finally the grains decrease even further in size for 6% anthraquinone content.

Although the crystallinity obtained by solvent casting (SAXS-WAXS) is higher than that obtained by cooling from the melt (DSC), interesting correlations can be established between the SAXS-WAXS and DSC experiments. From WAXS measurements, we conclude that the pendent group BP and AQ are not incorporated in the crystal. The expulsion of the pendent group before crystallization explain the shift of the crystallization exotherm measured in DSC. Due to their nonincorporation in the crystal, a high amount of modification (>6%) hinders the crystallization. For a low amount of modification (<1%), the decrease of the interplanar distance, the stability of the crystallinity, and the significant decrease of the Bragg peak width would indicate a

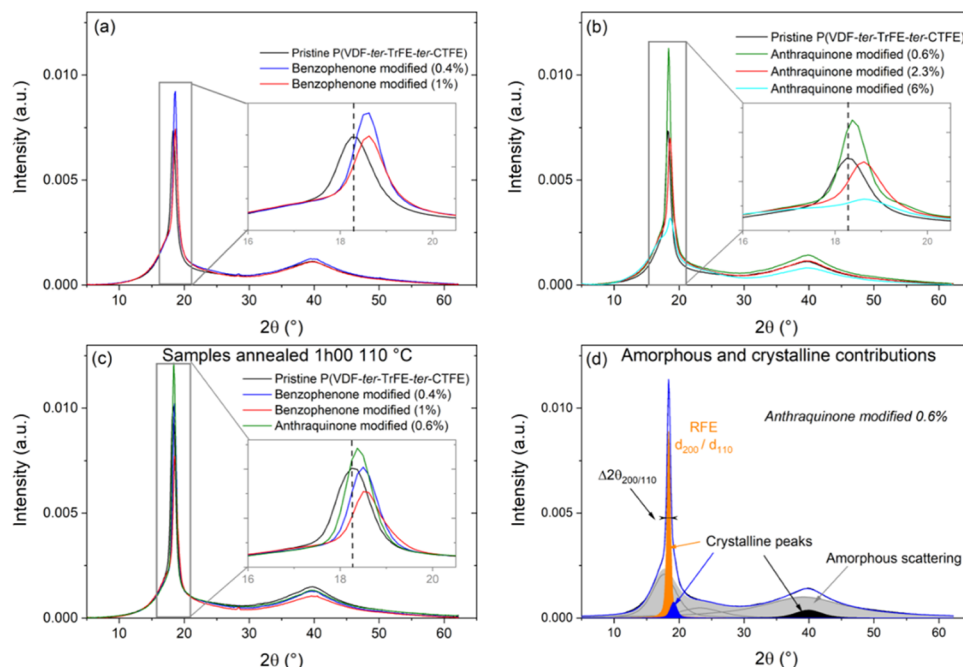


**Figure 3.** Evolution of the WAXS spectra for the modified fluorinated terpolymers for different contents of (a) benzophenone and (b) anthraquinone, (a, b) as cast and (c) after annealing at 110 °C for 1 h. An amplification on the main Bragg peak is shown in each picture (a–c). (d) WAXS spectra decomposition for the quantitative analysis; the amorphous phase appears in gray and the crystalline one in orange, blue, and black.

**Table 3. Summary of the Data Obtained by the Simultaneous SAXS–WAXS Experiments**

drop cast films	before annealing				after annealing, 1 h at 110 °C			
	$d$ (Å) <sup>a</sup>	$\Delta 2\theta$ (deg) <sup>a</sup>	$\chi_c$ (%)	$L_p$ (Å)	$d$ (Å) <sup>a</sup>	$\Delta 2\theta$ (deg) <sup>a</sup>	$\chi_c$ (%)	$L_p$ (Å)
pristine terpolymer	4.84	0.85	20	300	4.85	0.82	23	490 (240)
benzophenone 0.4%	4.77	0.7	21	250	4.79	0.7	24	490 (200)
benzophenone 1%	4.77	0.72	20	210	4.78	0.65	20	330 (175)
anthraquinone 0.6%	4.82	0.62	21	280	4.82	0.66	24	510 (250)
anthraquinone 2.3%	4.74	0.8	19	200				
anthraquinone 6%	4.74	1.1	9	150				

<sup>a</sup> $d$  is the interplanar distance associated with the Bragg peak (200)/(110) and  $\Delta 2\theta$  is their full width at half-maximum.

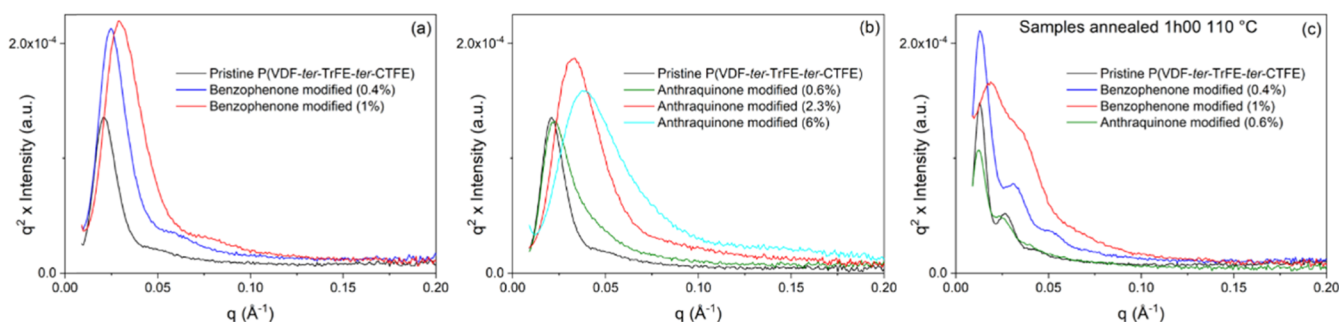


**Figure 4.** Evolution of the SAXS spectra for the fluorinated-modified terpolymers for different contents of (a) benzophenone and (b) anthraquinone, (a, b) as cast and (c) after annealing at 110 °C for 1 h.

perfection of the crystalline order in the plane of the crystalline lamellae, which can explain the observed thinning of the crystallization exotherm and the well-defined morphology observed by AFM. The decrease of the crystalline lamellae thickness explains the decrease in melting temperature.

**Photoresponsive Properties.** Self-standing films of the polymers grafted with benzophenone and anthraquinone

groups were characterized by UV–vis spectroscopy (Figure 6). Both polymers show strong deep UV absorption peaks; however, the terpolymer grafted with anthraquinone groups shows an additional i-line absorption peak.

As mentioned above, one of the reasons that the benzophenone and anthraquinone groups were chosen is that they act as type II photoinitiators. Thus, when polymers bearing these chromophores get exposed to UV light, triplet

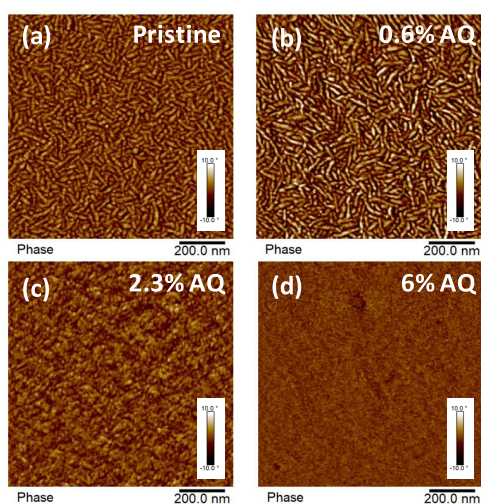


**Figure 5.** Phase AFM images of as-cast films of the pristine (a) and anthraquinone-modified P(VDF-*ter*-TrFE-*ter*-CTFE) terpolymers with various anthraquinone contents (b–d).

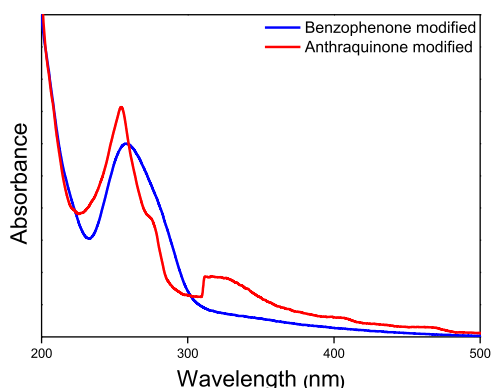


**Figure 6.** UV-vis absorption of self-standing films of P(VDF-*ter*-TrFE-*ter*-CTFE) modified with benzophenone (blue) and anthraquinone (red).

ketyl biradicals are reversibly formed by transferring of a nonbonding electron from the carbonyl oxygen to the carbonyl  $\pi^*$  orbital,<sup>23</sup> as described in Scheme 4. If the biradical does react during its half-life, the chromophore will return to its ground state and will be available for further excitation. However, if the ketyl biradical abstracts a

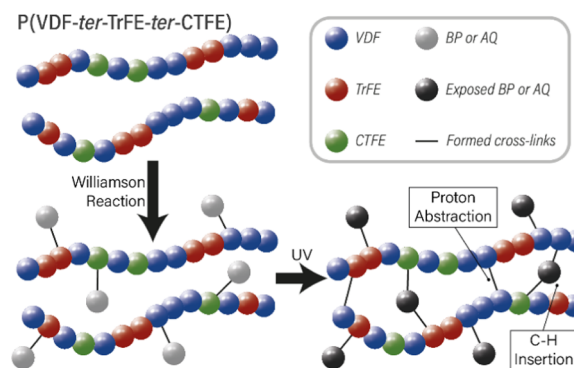


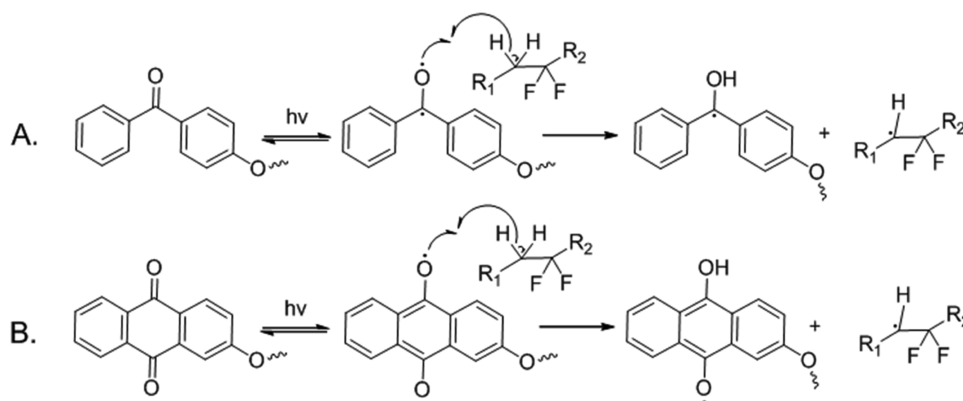
**Figure 7.** Schematic representation of the photoinduced cross-linking of P(VDF-*ter*-TrFE-*ter*-CTFE) polymers bearing either benzophenone or anthraquinone pendent groups.

hydrogen from a neighboring polymer chain, it will turn to a ketyl radical and a new alkyl radical will be formed on that chain. Subsequently, neighboring radicals can recombine, leading to the formation of a C–C bond and a cross-linked polymer network. Alternatively, the ketyl radicals can insert in C–H bonds (CHic-reaction), also leading to the formation of a cross-linked network,<sup>24</sup> as shown in Scheme 4. The cross-linking mechanisms are almost identical for both photoinitiators (Figure 7).

Photolithographic patterning processes were developed for fluoropolymers bearing both photoinitiators. The ultrahigh molar mass of the used polymers, with a polymerization degree greater than 2000, allows for very low cross-linker contents to be sufficient for an infinite network to be rapidly formed at a low UV dose. Optical microscopy images of the patterned films are shown in Figures S10 and S11.

**Dielectric and Ferroelectric Properties.** The impact of the different modification reactions on the dielectric properties was investigated by broadband dielectric spectroscopy at temperatures ranging from 20 to 80 °C. The real part of the relative permittivity ( $\epsilon'$ ) at 1 kHz of the terpolymers grafted with different contents of benzophenone (BP) and anthraquinone (AQ) was assessed in three different cases. First, the polymers were characterized as cast without any further treatment (Figure 8a,b), then similar films were annealed at 110 °C for 1 h and allowed to cool down slowly (Figure 8c,d), finally films were exposed at UV light, and then annealed (Figure 8e,f). It was observed that the

**Scheme 4.** Reversible Excitation of the Benzophenone (A) and Anthraquinone (B) Moieties upon Irradiation with UV Light and Subsequent Hydrogen Abstraction, Leading to the Formation of Free Radicals on the Polymer Backbone



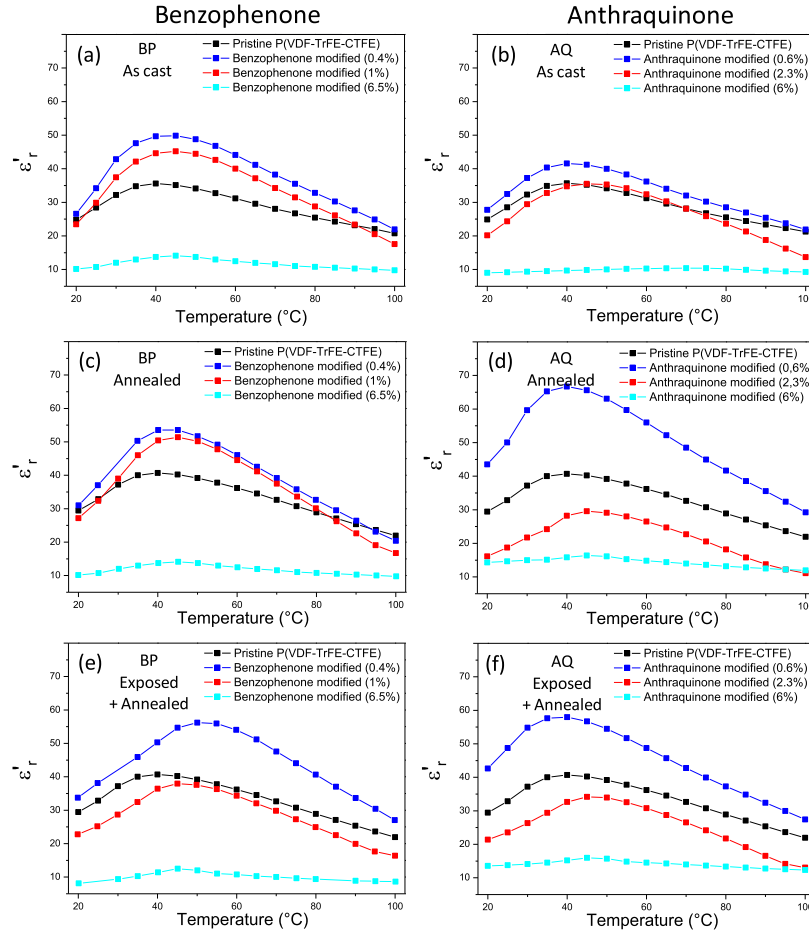


**Figure 8.** Real part of the relative permittivity (1 kHz) as a function of temperature for P(VDF-*ter*-TrFE-CTFE) functionalized with different contents of benzophenone (left) and anthraquinone (right) as cast (a, b), as annealed at 110 °C for 1 h (c, d), and after exposure to 6 J/cm<sup>2</sup> of UV light and subsequent annealing.

polymers grafted with low amounts of benzophenone (0.4%) and anthraquinone (0.6%) showed improved performance in terms of dielectric properties in all cases, while increasing either the benzophenone or the anthraquinone content leads to deteriorated properties. The highest observed enhancement in dielectric properties occurred for the annealed anthraquinone (0.6%) polymer, where a 60% increase in relative permittivity was observed at the peak temperature (40 °C), with the relative permittivity up to 65 compared to 40 for the pristine polymer. The annealing step was shown to improve the dielectric properties of all films; however, the largest improvement was again observed for this particular anthraquinone-modified polymer (0.6%) polymer, as shown in Figure 8. Exposure to UV light (6 J/cm<sup>2</sup>) was shown to have a negative impact on the dielectric properties of the various polymers (Figure 8e,f). However, despite the slight decrease in  $\epsilon'_r$  for the exposed films, the benzophenone (0.4%) and anthraquinone (0.6%) polymers still exhibited enhanced properties compared to the pristine P(VDF-*ter*-TrFE-CTFE), which was used as a reference.

A similar pattern was observed in the evolution of the ferroelectric properties with increasing the photoinitiator (PI) content. Again, the films were characterized in three steps, as cast (Figure 9a,b,e,f), after annealing (Figure 9c,d,g,h), and finally after exposure to UV light and subsequent annealing (Figure S12). Enhanced ferroelectric response was observed in all three steps of characterization for the low PI content

polymers. Grafting different groups was shown to have an impact on the ferroelectric character, with double hysteresis loop (DHL) behavior being observed for the pristine- and the anthraquinone-modified polymers. On the other hand, the benzophenone-modified polymers showed single hysteresis loop (SHL) behavior, which is an indicator of stronger pinning effect that inhibits the field-induced hysteresis caused by the relaxor-ferroelectric (RFE) to ferroelectric (FE) transition.

The annealing step had no great impact on the ferroelectric properties, contrary to the dielectric properties, where the impact was much more pronounced. At high PI contents, the polymers behave as linear dielectrics, as the crystallinity is very low, causing most of the dipoles to be located in the amorphous lattice and thus not to interact with each other, giving rise to almost zero hysteresis, a characteristic of linear dielectrics.

## CONCLUSIONS

A general method enabling the introduction of additional functionality to FEPs was developed in this work. Relaxor-ferroelectric P(VDF-*ter*-TrFE-CTFE) polymers were functionalized with photoinitiator groups via a simple etherification reaction, and the produced cross-linkable polymers exhibited in some cases enhanced electroactive properties even when compared to the state-of-the-art pristine polymers.

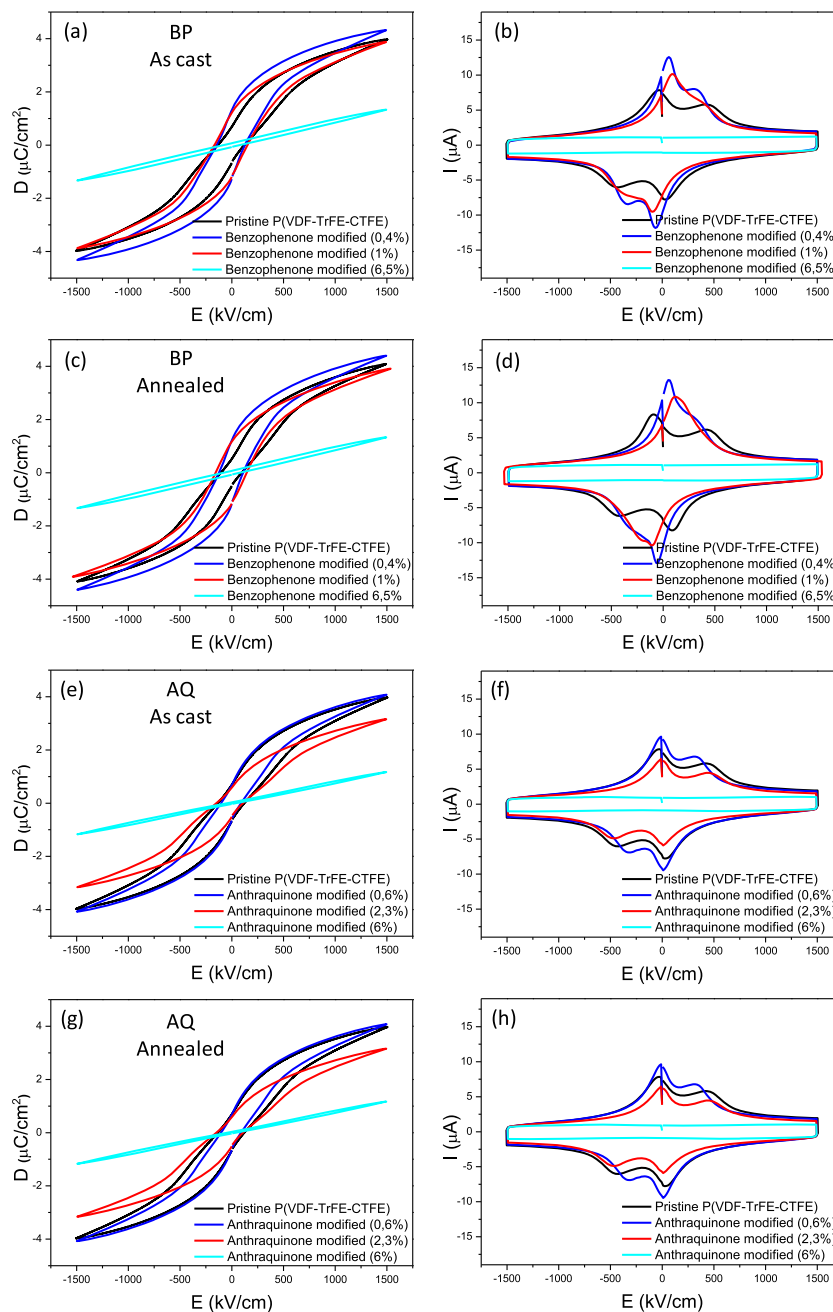


**Figure 9.** Ferroelectric testing at room temperature of P(VDF-*ter*-TrFE-*ter*-CTFE) functionalized with different contents of benzophenone (BP) and anthraquinone (AQ), before and after annealing at 110 °C for 1 h: displacement (left) and current (right).

The enhancement in terms of relative permittivity was as much as 60% for the anthraquinone (0.6%) containing polymer, where the dielectric constant increased from 40 to 65 at 40 °C. This property enhancement was attributed to the perfection of the crystalline order, expressed by the decrease of the interplanar distance and the Bragg peak width. Despite this method being used in the context of this report primarily to induce photopatternability and tune the electroactive properties of FEPs, it is by no means limited to such use, as it allows for the grafting of different functional groups in different kinds of fluorinated polymers.

Figure S1,  $^{19}\text{F}$  NMR at 376.5 MHz of benzophenone-grafted P(VDF-*ter*-TrFE-*ter*-CTFE) terpolymer; Figure S2, SEC in DMF of the pristine- and the benzophenone-grafted P(VDF-*ter*-TrFE-*ter*-CTFE) terpolymer with 6.5% benzophenone content; Figure S3,  $^{19}\text{F}$  NMR at 376.5 MHz of anthraquinone-grafted P(VDF-*ter*-TrFE-*ter*-CTFE) terpolymer; Figure S4, SEC in DMF of the pristine- and the anthraquinone-grafted P(VDF-*ter*-TrFE-*ter*-CTFE) terpolymer with

0.6% anthraquinone content; Figure S5, thermal gravimetric analysis of the pristine- and the anthraquinone-grafted P(VDF-*ter*-TrFE-*ter*-CTFE) terpolymer with 0.6% anthraquinone content; Figure S6, FT-IR spectra of 4-hydroxy benzophenone; Figure S7, FT-IR spectra of 2-hydroxy anthraquinone; Figure S8, optical microscope picture of patterned benzophenone-modified P(VDF-*ter*-TrFE-*ter*-CTFE) terpolymer; Figure S9, optical microscope picture of patterned anthraquinone-modified P(VDF-*ter*-TrFE-*ter*-CTFE) terpolymer; Figure S10, ferroelectric testing at room temperature of P(VDF-*ter*-TrFE-*ter*-CTFE) functionalized with different benzophenone and anthraquinone contents ([PDF](#))

## AUTHOR INFORMATION

### Corresponding Author

\*E-mail: [Georges.Hadziioannou@u-bordeaux.fr](mailto:Georges.Hadziioannou@u-bordeaux.fr).

### ORCID

Thibaut Soulestin: 0000-0002-1534-0230

Cyril Brochon: 0000-0003-3242-1574

Eric Cloutet: 0000-0002-5616-2979

Georges Hadziioannou: 0000-0002-7377-6040

### Author Contributions

All authors have given approval to the final version of the manuscript.

### Notes

The authors declare no competing financial interest.

## ACKNOWLEDGMENTS

The authors acknowledge the financial support from Arkema and Région Aquitaine as well as from the Industrial Chair (Arkema/ANR) within the grant agreement no. AC-2013-365. K.K. acknowledges the Région Aquitaine for the financial support (Ph.D. grant #2015-1R10207-00004862). This work was performed within the framework of the Equipex ELORPrintTec ANR-10-EQPX-28-01 with the help of the French state's Initiative d'Excellence IdEx ANR-10-IDEX-003-02. S.T.-G. contribution was achieved within the framework of the Industrial Chair Arkema (Arkema/CNRS-ENSAM-CNAM).

## ABBREVIATIONS

$k$ , dielectric constant; FEP, fluorinated electroactive polymer; OFET, organic field-effect transistor;  $\epsilon'$ , real part of the relative permittivity;  $\tan \delta$ , dielectric loss; BP, benzophenone; AQ, anthraquinone; PI, photoinitiator

## REFERENCES

- (1) MacDiarmid, A. G. "Synthetic Metals": A Novel Role for Organic Polymers (Nobel Lecture). *Angew. Chem., Int. Ed.* **2001**, *40*, 2581–2590.
- (2) Facchetti, A.  $\pi$ -Conjugated Polymers for Organic Electronics and Photovoltaic Cell Applications. *Chem. Mater.* **2011**, *23*, 733–758.
- (3) Soulestin, T.; Ladmiral, V.; Dos Santos, F. D.; Ameduri, B. Vinylidene fluoride- and trifluoroethylene-containing fluorinated electroactive copolymers. How does chemistry impact properties? *Prog. Polym. Sci.* **2017**, *72*, 16–60.
- (4) Lovinger, A. J. Ferroelectric polymers. *Science* **1983**, *220*, 1115–1121.
- (5) Zhang, Q. M.; Bharti, V.; Zhao, X. Giant Electrostriction and Relaxor Ferroelectric Behavior in Electron-Irradiated Poly(vinylidene

fluoride-trifluoroethylene) Copolymer. *Science* **1998**, *280*, 2101–2104.

(6) Terzic, I.; Meereboer, N. L.; Acuautila, M.; Portale, G.; Loos, K. Electroactive materials with tunable response based on block copolymer self-assembly. *Nat. Commun.* **2019**, *10*, No. 1600460.

(7) Meereboer, N. L.; Terzic, I.; van der Steeg, P.; Portale, G.; Loos, K. Physical pinning and chemical crosslinking-induced relaxor ferroelectric behavior in P(VDF-*ter*-TrFE-*ter*-VA) terpolymers. *J. Mater. Chem. A* **2019**, *7*, 2795–2803.

(8) Abusleme, J. A.; Maccone, P. Polymerization process in aqueous emulsion of fluorinated olefinic monomers. Google Patents, US5516863A, 1996.

(9) Dos Santos, F. D.; Lannuzel, T. Method for preparation of derivatives of polyvinylidene fluoride. Google Patents, WO2016055712A1, 2017.

(10) Guan, F.; Wang, J.; Yang, L.; Tseng, J.-K.; Han, K.; Wang, Q.; Zhu, L. Confinement-Induced High-Field Antiferroelectric-like Behavior in a Poly(vinylidene fluoride-co-trifluoroethylene-co-chlorotrifluoroethylene)-graft-polystyrene Graft Copolymer. *Macromolecules* **2011**, *44*, 2190–2199.

(11) Guan, F.; Yang, L.; Wang, J.; Guan, B.; Han, K.; Wang, Q.; Zhu, L. Confined Ferroelectric Properties in Poly(Vinylidene Fluoride-co-Chlorotrifluoroethylene)-graft-Polystyrene Graft Copolymers for Electric Energy Storage Applications. *Adv. Funct. Mater.* **2011**, *21*, 3176–3188.

(12) Rahimabady, M.; Qun Xu, L.; Arabnejad, S.; Yao, K.; Lu, L.; Shim, V. P.; Gee Neoh, K.; Kang, E.-T. Poly (vinylidene fluoride-co-hexafluoropropylene)-graft-poly (dopamine methacrylamide) copolymers: A nonlinear dielectric material for high energy density storage. *Appl. Phys. Lett.* **2013**, *103*, No. 262904.

(13) Kallitsis, K.; Thuau, D.; Soulestin, T.; Brochon, C.; Cloutet, E.; Dos Santos, F. D.; Hadziioannou, G. Photopatternable High-k Fluoropolymer Dielectrics Bearing Pendant Azido Groups. *Macromolecules* **2019**, *52*, 5769–5776.

(14) Bargain, F.; Thuau, D.; Panine, P.; Hadziioannou, G.; Domingues Dos Santos, F.; Tencé-Girault, S. Thermal behavior of poly(VDF-*ter*-TrFE-*ter*-CTFE) copolymers: Influence of CTFE monomer on the crystal-crystal transitions. *Polymer* **2019**, *161*, 64–77.

(15) Boschet, F.; Ameduri, B. (Co)polymers of Chlorotrifluoroethylene: Synthesis, Properties, and Applications. *Chem. Rev.* **2014**, *114*, 927–980.

(16) Kise, H.; Ogata, H.; Nakata, M. Chemical dehydrofluorination and electrical conductivity of poly(vinylidene fluoride) films. *Angew. Makromol. Chem.* **1989**, *168*, 205–216.

(17) Kallitsis, K. J.; Nannou, R.; Andreopoulou, A. K.; Daletou, M. K.; Papaioannou, D.; Neophytides, S. G.; Kallitsis, J. K. Crosslinked wholly aromatic polyether membranes based on quinoline derivatives and their application in high temperature polymer electrolyte membrane fuel cells. *J. Power Sources* **2018**, *379*, 144–154.

(18) Kim, J.; Hanna, J. A.; Byun, M.; Santangelo, C. D.; Hayward, R. C. Designing responsive buckled surfaces by halftone gel lithography. *Science* **2012**, *335*, 1201–1205.

(19) Schwärzle, D.; Hou, X.; Prucker, O.; Rühle, J. Polymer Microstructures through Two-Photon Crosslinking. *Adv. Mater.* **2017**, *29*, No. 1703469.

(20) Li, M.; Wondergem, H. J.; Spijkman, M.-J.; Asadi, K.; Katsouras, I.; Blom, P. W. M.; de Leeuw, D. M. Revisiting the  $\delta$ -phase of poly(vinylidene fluoride) for solution-processed ferroelectric thin films. *Nat. Mater.* **2013**, *12*, 433.

(21) Yang, L.; Li, X.; Allahyarov, E.; Taylor, P. L.; Zhang, Q. M.; Zhu, L. Novel polymer ferroelectric behavior via crystal isomorphism and the nanoconfinement effect. *Polymer* **2013**, *54*, 1709–1728.

(22) Bargain, F.; Panine, P.; Dos Santos, F. D.; Tence-Girault, S. From solvent-cast to annealed and poled poly (VDF-co-TrFE) films: New insights on the defective ferroelectric phase. *Polymer* **2016**, *105*, 144–156.

(23) Preston, G. W.; Wilson, A. J. Photo-induced covalent cross-linking for the analysis of biomolecular interactions. *Chem. Soc. Rev.* **2013**, *42*, 3289–3301.

(24) Körner, M.; Prucker, O.; Rühle, J. Kinetics of the Generation of Surface-Attached Polymer Networks through C, H-Insertion Reactions. *Macromolecules* **2016**, *49*, 2438–2447.